



Polycaprolactone-blended cellulose acetate thin-film composite membrane for dairy waste treatment using forward osmosis

Akash M. Chandran¹ · Ekta Tayal¹ · Prasanna Kumar S. Mural²

Received: 28 December 2021 / Accepted: 10 May 2022 / Published online: 17 May 2022
© The Author(s), under exclusive licence to Springer-Verlag GmbH Germany, part of Springer Nature 2022

Abstract

In recent years new sustainable technology for wastewater treatment has emerged, and among them, forward osmosis (FO) has gained importance. FO utilizes osmotic pressure difference across the semipermeable membrane as the driving force to concentrate the wastewater. Further, the surface and physical properties of the semipermeable FO membrane play a crucial role during the FO process in reducing the internal concentration polarization. In general, FO membranes are prepared using cellulose acetate (CA) polymer due to their high hydrophilic nature. However, CA membranes are mechanically unstable for the FO process. Hence, to increase the mechanical strength and flexibility of CA, other polymers are blended along with it. In this present study, we have prepared a phase-inversion membrane using CA blended with polycaprolactone (PCL) polymers. Further, to increase the hydrophilicity of the membrane, a thin-film composite (TFC) layer of polyamide is coated using interfacial polymerization. To increase the antifouling properties of the membrane, graphene oxide (GO) and copper oxide (CuO) nanoparticles (NPs) are incorporated inside the TFC matrix. The prepared NPs and membrane were characterized using Fourier-transform infrared spectroscopy (FTIR), wide-angle X-ray scattering (WAXD), and contact angle. Further, the GO-CuO incorporated TFC coating has improved the hydrophilicity and antifouling properties of the membrane. It was observed that the water flux has increased up to 5 LMH, and reverse solute flux has reduced to 4 GMH. Further, the membrane was utilized to concentrate in situ prepared dairy waste. It was observed that after 60 min of the FO process, the concentration of dairy waste had increased to 23%, with a concentration factor of 0.903. Thus, a prepared TFC phase inversion membrane is potential for dairy wastewater treatment.

Keywords Cellulose acetate · Polycaprolactone · Polymer blends · Phase inversion · Thin-film composite · Graphene oxide · Copper oxide

Introduction

The essential contribution to sustaining a healthy environment is water. Through works, it has been established that about two-thirds of the Earth's surface is enclosed with water, out of which only 2.5% is fresh water, and an unbiased

0.3% is accessible for human consumption. The increase in population, industrialization, and improved living standards has upsurged the demand for freshwater, thereby making people aware of its importance and vulnerability in terms of quality. This issue can be addressed by incorporating a proper wastewater treatment methodology. The traditional wastewater treatment approaches include filtration, coagulation-flocculation, or biological treatment (Badawi and Zaher 2021). However, among these various methods, the most acknowledged technique is membrane technology. Membrane technology has shown significant progress in the last decades owing to its easy accessibility and environmental friendliness. Several membrane processes that have been tried earlier for treating wastewater are ultrafiltration (UF), microfiltration (MF), nanofiltration (NF), membrane distillation (MD), and RO (Tufa et al. 2019). Amongst these, RO has received a greater appreciation for water reclamation due

Responsible Editor: Angeles Blanco

✉ Prasanna Kumar S. Mural
prasannamural@iitb.ac.in

¹ Materials Chemistry and Polymer Technology Group, Department of Chemical Engineering, National Institute of Technology Calicut, Kozhikode, Kerala 673601, India

² Department of Metallurgical Engineering & Materials Science, Indian Institute of Technology Bombay, Powai, Mumbai 400076, India

to its higher efficiency. This technology was anticipated to bridge the gap between economics and sustainability (Obaid et al. 2016).

Dairy processing is now one of the largest sources of industrial wastewater due to rapid industrialization. Approximately 60–80% of the water consumed in the industry is contaminated (Chandra et al. 2018). The production of several food items from raw milk resulted in the formation of a diverse runoff stream with qualitative and quantifiable variations, which is restricted for further reuse. The primary characteristics of dairy wastewater are high temperature, high organic content, and a wide pH range (Ayeche 2012; Slavov 2017). To avoid environmental damage, the wastewater from the dairy industries must be treated. Milk production results in the production of wastewater containing similar constituents. The type of treatment required is heavily influenced by the composition and flow rate of the wastewater. Because of the high energy requirements and significant fouling of membranes, pressure-driven membrane processes (RO) cannot be used to treat this contaminated water. Also, this pressure-driven process entails a large energy requirement and is costly. A new energy-efficient technique, forward osmosis (FO), was introduced to encounter water stresses cautiously. The FO process has the advantage of high pollutants rejection without the need for considerable hydraulic pressure to operate the system. This procedure, among other things, can concentrate low-strength wastewater and thereby increase the nutrients extracted from it, which can then be utilized as fertilizer in agriculture (Cath et al. 2006; Xue et al. 2015).

Forward osmosis is an evolving energy-efficient membrane separation technology proposed in the 1970s. It trails the natural phenomenon of osmosis, involving the passage of water crossways toward the membrane from the low concentration region, known as feed solution, to the high concentration region, known as draw solution (Cath et al. 2006). This movement of water molecules across the membrane is due to the osmotic pressure gradient between the two solutions. The main advantage of FO is that it does not require any external pressure, which aids in the minimal fouling of membranes in comparison to other pressure-driven processes that are already in use (Pramanik et al. 2019). As discussed early, the FO is a nonpressure-driven process. Hence, the research and development of FO membranes are still in their early stages. The search for acceptable membranes is a new topic with a wide range of applications in water and wastewater treatment. The appropriate membrane material and membrane-forming method are critical for membrane efficiency. Polymer membrane material should be chemically resistant and produce polymer films with excellent mechanical strength.

Since the phase-inversion methodology was invented for fabricating asymmetric polymeric membranes by Loeb and Sourirajan more than 40 years ago, cellulose acetate (CA) has been a popular material for numerous separation

applications (Loeb and Sourirajan 1963; Zhang et al. 2010). It has distinct characteristics such as relative hydrophilicity, which favors high water flux and low fouling tendency, as well as extensive availability and low toxicity. Also, CA polymers are low prices and have moderate chlorine resistance (Liu et al. 2016). However, CA membranes are not mechanically or thermally stable, which limits their application. To overcome this problem, CA polymer is blended with other polymers to enhance its overall properties. Early CA polymer was blended with cellulose triacetate (CT) for FO applications that have low permeate water flux because their porous support layer causes a high internal concentration polarization due to their porous support layer.

Similarly, to improve the mechanical properties, Tabinda et al. have blended CA with polyurethane (PU), which enhanced the membrane's mechanical stability and formation ability (Riaz et al. 2016). All of these membranes suffer from severe internal concentration polarization (ICP), which severely limits the effective driving force due to their nonselective and low-porosity support layers. Hence, to enhance the water flux and reduce ICP, the CA FO membrane was used with TFC membranes. This took the FO platform to show an enhanced water flux performance and better salt rejection. The currently used FO membranes are designed by forging a thin-film polymerization over the base membrane as a support layer. Optimization studies conducted on the TFC membranes reported that a base layer with a mixture of different morphologies greatly affected the membrane performance. The synthesis of chemically stable high-performance FO membranes is still in its early phases of development. The unique advantages offered by CA make it worthwhile to investigate further into its improvement that might have been unnoticed in the past. Therefore, the phase inversion of CA polymers should be investigated further in order to discover new progress that may have been overlooked in the past but which can be a useful supplement to traditional theories and in order to search for a better membrane structure for FO processes in order to achieve the ultimate goal of water remediation. New studies and advancements in the TFC membranes recommend producing a thin porous support layer for vindicating the effect of ICP, thereby sustaining the top dense selective layer for effective water flux.

In this present study, we have enhanced the mechanical properties of the CA membrane by blending the CA polymer with the PCL polymer. PCL is a synthetic biodegradable polymer. It is a significant polymer due to its mechanical qualities (great strength and elasticity) and miscibility with a wide range of other polymers (Maio et al. 2020). Also, it is the most hydrophobic polymer with high stability (Zhang et al. 2019). Due to its high miscibility, it has been used to blend with other polymers to improve the properties of the membrane. The present study approach includes

(1) incorporating PCL into CA to enhance its mechanical strength drastically. (2) The presence of PCL can be tailored accordingly to the hydrophilicity needs of the support layer for reducing the ICP. Blending CA with PCL retains the biodegradable properties of the membrane. (3) No study has reported this combination (CA-PCL) for preparing FO membranes so far. Further, to enhance the hydrophilicity and reduce ICP, the CA-PCL membrane was coated with a polyamide layer (selectivity layer) over the surface. Also, the antifouling properties were further enhanced by incorporating GO and CuO NPs. Hence, the potential benefit of low fouling of prepared membrane was utilized to concentrate dairy wastewater.

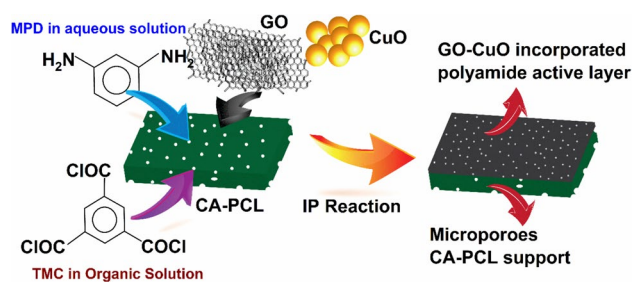
Materials and method

Preparation of nanoparticles

Graphene oxide is prepared using the modified hummers method (Chandran et al. 2021b). In general, 2 g of graphite was washed subsequently with water and ethanol to remove any contamination. Further, the graphite (sigma) was oxidized using a mixture of H_2SO_4 and H_3PO_4 (9:1, Merck India) with the appropriate amount of $KMnO_4$ (Merck India) and stirred at 60 °C for 12 h. After the oxidation reaction, the acid slurry was poured into an ice-cold distilled water with 20% H_2O_2 (Merck India). The yellow color appeared to confirm the formation of GO NPs. Further, the yellow-colored suspension was separated and washed using distilled water and ethanol subsequently. The obtained mass after washing was dried in a vacuum oven at 60 °C. Similarly, the CuO was prepared using the sole gel method (Etefagh et al. 2013). To prepare the precursor, an appropriate amount of copper nitrate (99.9%, Merck India) was added to a mixture of ethanol and water (1:1). The citric acid (99.9% Merck India) was used as the reducing agent and ethylene glycol as the stabilizer. The mixture refluxed for 4 h at 100 °C, and the obtained black powder was calcinated at 600 °C.

Preparation of FO membrane

The membrane was cast using the phase-inversion method (Chandran et al. 2021a). In general, 18 wt.% of cellulose acetate (CA-Sigma-Aldrich Mn ~ 50,000 (by GPC) and ~40% acetyl.) was dissolved in an approximate volume of DMF (Merck India) and acetone (Merck India) (7:3). After 4 h of stirring, the polymer solution was poured over the glass substrate, cast using a doctor's blade, and immersed in a water bath for membrane precipitation. To remove the solvent, the precipitated membrane was washed with DI water. Similarly, a CA-PCL blend membrane with 20 wt.% of polycaprolactone (PCL-average M_n 80,000, Sigma-Aldrich) was



Scheme 1 Fabrication of GO-CuO-doped TFC CA-PCL blend polymer membrane

fabricated using a similar method. To increase the hydrophilicity of the membrane, an interfacial polymerization (IP) process was used to form a polyamide selective layer on the upper surface of the CA-PCL membrane. The IP reaction was carried out using m-phenylenediamine (MPD, 99% Sigma-Aldrich) and 1,3,5-benzenetricarbonyl trichloride (TMC 99%, Sigma-Aldrich). The as-prepared CA-PCL membrane was kept on a glass plate and a 2.0 wt.% MPD aqueous solution was emptied over it. The poured solution was then reserved for 2 min to ensure proper saturation, followed by careful removal of excess solution. Following the drying of the aqueous solution, the top surface of the membrane was brought into contact with a 0.1 wt.% TMC/n-hexane solution for 1 min. The resultant CA-PCL-TFC (thin-film composite) membrane was washed and stored in DI water after drying at room temperature for several minutes and then in the oven for 20 min at 70 °C. The thin-film nanocomposite (TFN) membrane was prepared using GO and CuO. The MPD solution with varying concentrations of GO wt.% (0, 0.005, 0.01, 0.02) was taken, followed by TMC, the solution for the preparation of TFN. The prepared TFN membranes were named CP0.005, CP0.01, and CP0.02, respectively. Similarly, prepared CuO NPs were incorporated in TFN as depicted in Scheme 1. The fabricated membrane was named CP (CA-PCL membrane), CPT (thin-film composite membrane), CPTG (graphene-doped CA-TFC membrane), and CPTGA (CuO NP-doped graphene CA-TFC).

Characterization

The morphology of NPs was investigated using FESEM (model: Gemini SEM 300 Brand: Carl Zeiss). Surface functionality and crystallinity were studied using FTIR (PerkinElmer Frontier MIR) and WAXD (PANalytical). Structure defects of GO were investigated using Raman spectroscopy (532-nm laser-Horiba Labram HR Evo). The blend formation of CA-PCL was investigated using FTIR (PerkinElmer Frontier MIR) and WAXD (PANalytical). The water contact angle of the membrane was measured (Kyowa, DMS-401, Japan) to gain a piece of knowledge about the hydrophilicity

of the membranes. The contact angles conveyed are an average of five measurements done at different locations on the individual membrane samples. Information regarding the mechanical stability, tensile strength, and percentage elongation of the membrane was obtained using Universal Testing Machine (UTM-Shimadzu, AG-X plus, Japan).

Performance of membrane

The performance evaluation of the membrane is made using a lab-scale FO setup. The FO arrangement involves a cross-flow cell, two pumps for the circulation of individual feed and draws solutions, respectively, and a weighing balance on both sides to measure the amount of water passed. The effective area of the FO cell used is $150 \times 100 \text{ mm}^2$. Spacers were used along with the membrane in the cell to increase the mass flow rate. The membrane performance is evaluated in the AL-FS mode, i.e., where the selective polyamide layer of the membrane faces the feed side. The forward osmosis tests were conducted using DI water as the feed solution and NaCl as the draw solution. The hydraulic pressures of both solutions were the same ($< 1.0 \text{ kg/cm}^2$). Volumetric flow rates through the cell were maintained at 40 L/h . Initial volumes of feed and draw solution were 3 L and 1 L , respectively. After the start of the process, the changes in the weight on both sides were recorded. If the feed side, in any case, shows an increase in weight, then the process should be stopped immediately. Otherwise, the process is continued for a certain period until a constant conductivity value of

the feed solution is observed. The water flux J_w ($\text{Lm}^{-2} \text{ h}^{-1}$) through the membrane is calculated using the equation.

$$J_w = \frac{\Delta V}{S \Delta t} \quad (1)$$

where ΔV (in liters) is the volume change of the feed solution, S (in m^2) is the area of the membrane available for flux (in $\text{Lm}^{-2} \text{ h}^{-1}$), and Δt (in hours) is the time interval during which the volume changes by amount ΔV . During each run, volumes of the draw solution were documented before and after testing. A graph was plotted for feed solution representing its conductivity against the concentration. This change in conductivity of the feed solution for each run was used to evaluate the reverse salt flux (J_s , $\text{gm}^{-2} \text{ h}^{-1}$, GMH) of the draw solution.

$$J_s = \frac{\Delta C_t * V}{\Delta t * A_m} \quad (2)$$

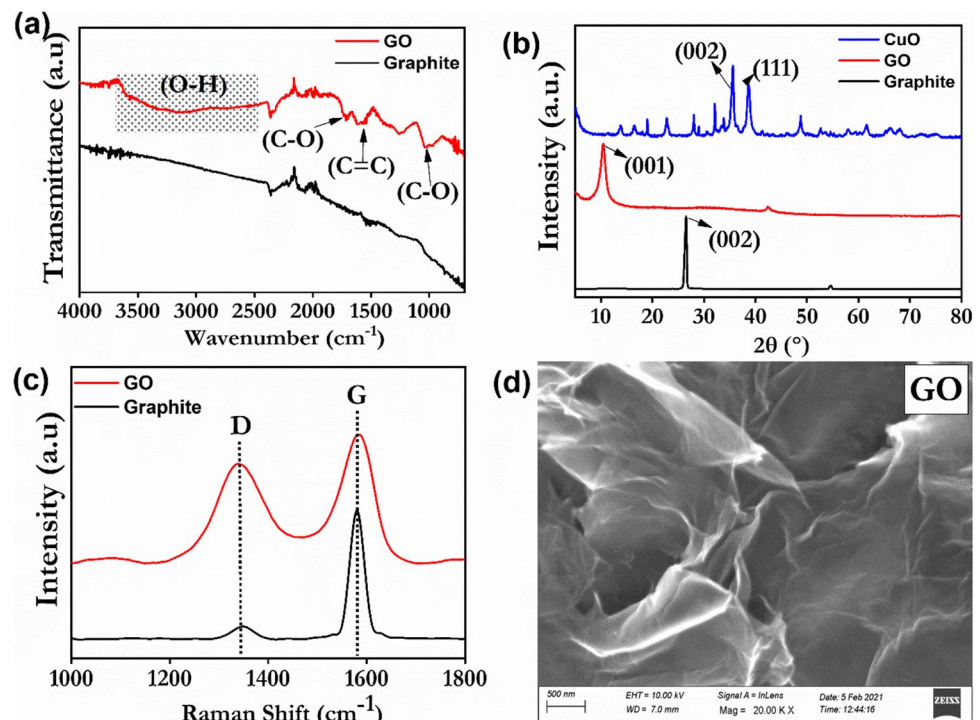
where ΔC_t (g/L) is the changes in salt concentration, and V (L) is the feed solution volume.

Result and discussion

Nanoparticles

The FTIR spectrum of graphite and GO is depicted in Fig. 1a, and the broadening of the peak for GO in a range of

Fig. 1 **a** FTIR spectrum graphite and GO, **b** WAXD of CuO, graphite and GO, **c** Raman spectrum of graphite and GO, and **d** FESEM of GO



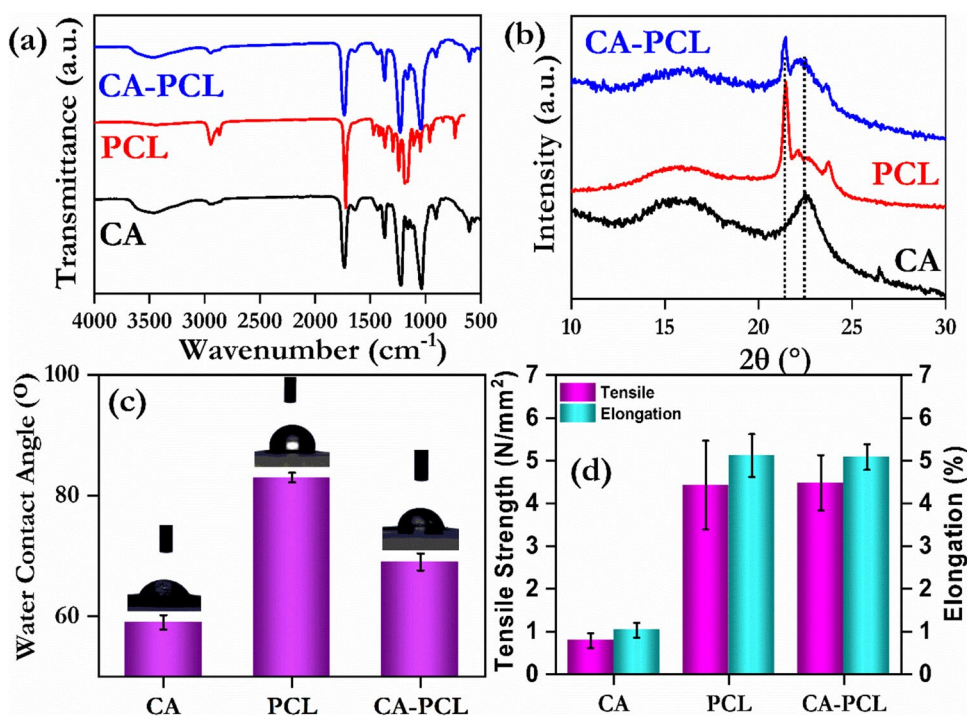
3000–3500 cm^{-1} is attributed to the stretching vibration of the hydroxy group (O–H). Further, the new peaks observed for GO at 1726, 1626, and 1040 cm^{-1} correspond to C–O and C=O bonds of the carboxyl group (Mural et al. 2015). This confirms the formation of hydrophilic GO formation. Figure 1b shows the WAXD of prepared GO and CuO. The CuO NPs has shown the characteristic peak at 35.62° and 38.62°, which corresponds to the (002) and (111) plane of CuO NPs. Similarly, graphite has shown the characteristic peak at 26.53°, which corresponds to the (002) plane. Further, the GO NPs have shown a characteristic peak at 10.45°, which attribute to the (001) plane of GO. This shift in WAXD indicates the formation of GO NPs. Further, Fig. 1c corresponds to the Raman spectroscopy of graphite and GO NPs. The peak observed at ~1580 and 1348 cm^{-1} for graphite corresponds to the G and D bands. The G band is attributed to the sp^2 domain of graphite, and the D band corresponds to defects present. It is observed from Fig. 1c that the intensity of the D band has increased for GO compared to graphite. This indicates intense oxidation of graphite to GO (Chandran et al. 2021b). The surface morphology of GO NPs showed a sheet-like structure with curved edges, as depicted in Fig. 1d.

Membrane characterization

The FTIR spectrum, as depicted in Fig. 2a of pristine CA, showed a typical adsorption band at 1732 cm^{-1} , 1368 cm^{-1} , 1229, and 1034 cm^{-1} , which attributed to the C=O, $-\text{CH}_2$ and C–O–C vibration from the acetyl group,

respectively (Joshi et al. 2015). Similarly, the FTIR spectrum for pristine PCL shows the characteristic peaks at 2943 and 2864 cm^{-1} attributing to the stretching band of the CH_2 group in the polymer chain. Further, for PCL, the asymmetric deformation and symmetric wagging of CH_3 are observed at 1472 and 1366 cm^{-1} bands. The asymmetric and symmetric stretching of C–O–C and C–O is also observed in 1294, 1163, and 1108 cm^{-1} bands. The CA-PCL blends showed steady alteration in FT-IR peaks. It is observed from the FTIR spectrum of the CA-PCL blend that the characteristic peak intensity of CA observed at 1229 and 1034 cm^{-1} has gradually increased with the addition of PCL polymer; also, a measured shift in the peaks was observed. Similarly, the characteristic peak observed at 1732 cm^{-1} , which corresponds to C=O, has shifted to a lower value. These results indicated that the PCL has effectively interacted with CA to form a blend (He et al. 2021). Khoshnevisan et al. have fabricated a CA-PCL blend membrane using electrospinning technology. They observed similar characteristic peaks of ether (1043 cm^{-1}), ester (1234 cm^{-1}), and carbonyl (1369 cm^{-1}) group, which confirm the blend formation (Khoshnevisan et al. 2019). Similarly, Joshi et al. fabricated CA-PCL electrospun blend, and the blend formation was confirmed using FTIR spectroscopy. The necessary shift in the peaks was observed in the blend, which confirmed the CA-PCL blend formation (Joshi et al. 2015). Similarly, Fig. 2c corresponds to the WAXD of CA, PCL, and CA-PCL. It is observed that CA has shown only a prominent peak at 22.5°, which attributes to the (200) plane of cellulose II

Fig. 2 a FTIR spectrum, b WAXD, c water contact angle, and d tensile and elongation of CA, PCL, and CA-PCL membrane



structure (Rouhani and Fashandi 2018). Also, the WAXD of CA indicates lower crystallinity. Similarly, neat PCL has shown the characteristic peak at 21.45°, 22°, and 23.8°, which corresponds to the (110), (111), and (200) planes of orthorhombic crystalline PCL (Sun et al. 2018). Further, the WAXD peak of CA-PCL has shown both peaks at 21.45° and 22.19° indicating the CA-PCL blend formation (Palacios Hiestroza et al. 2020). Figure 2c corresponds to the measured water contact angle; it can be seen that the contact angle of pristine CA is ~59°, which characterizes the hydrophilic nature of the polymer. Blending the hydrophobic PCL polymer (contact angle ~83.69°) into CA, increases its contact angle to 69.7°, thereby decreasing its hydrophilicity by 16.67%. The tensile strength and percentage elongation of the prepared neat and blend membrane are depicted in Fig. 2d. Three samples were tested for each individual CA, PCL, and CA-PCL membrane, and an average value was estimated and compared. From Fig. 2d, it is observed that the tensile strength of neat CA is very less as compared to the PCL, demonstrating its lower resistance to deformation. The subsequent blending of PCL in the neat CA to obtain the CA-PCL membrane exhibits a drastic improvement in its tensile strength. Also, the results display that blending has increased the elastic behavior of pristine CA by 395%. With the use of this CA-PCL blended membrane in the forward osmosis process, it is possible to address the mechanical stability issue caused by the pristine CA membrane.

As discussed early, the blending of PCL polymer will enhance the mechanical properties of CA polymer. However, the hydrophilicity of the membrane decreases due to the hydrophobic nature of PCL. To overcome this, a thin-film layer of polyamide is coated over the CA-PCL blend. Also, GO, and CuO NPs were incorporated inside the thin film to form a thin-film nanocomposite. The FTIR spectrum was employed to investigate molecular-level interaction. The FTIR spectrum, as depicted in Fig. 3a, corresponds to phase-inversion CP, CPT, CPTG, and CPTGC membrane. It is observed from Fig. 3a that the phase-inversion CP and CPT membrane has comparable peaks. The TFC-coated

CPT membrane has shown new peaks at 1649, 1611, and 1541 cm^{-1} attributed to the N–H bending aromatic amide ring and C = O stretching in the –CO–NH– group, correspondingly (Park et al. 2017).

Further, the peak located at 1661 cm^{-1} in the CPTG membrane is associated with the C = O stretching of the carbonyl group. This spectrum confirms the formation of new amide bonds between the NH_2 group of MPD and OH groups of the GO. Further, there can be observed the presence of a new peak at 700 cm^{-1} , and a subsequent shift in the range of 1200 cm^{-1} can be attributed to the presence of copper oxide. The relative hydrophilicity of both the polyamide-coated and nanoparticle-incorporated membrane was measured by the contact angle shown in Fig. 3b. Time-dependent measurement of water contact angle demonstrates that the nanoparticles doped membranes; CPTGC have a better wettability than the CP membrane. The amalgamation of nanoparticles has reduced the contact angle of the CPT membrane from ~67 to 32°, thus increasing its hydrophilicity by 52%. This increase in the hydrophilic property of the membrane was desired to reduce the antifouling behavior and increase the water flux performance.

Membrane performance

The prepared CPT membrane was tested for different concentrations of draw solute (0.1, 0.5, and 1 M of NaCl with osmotic pressure of 5, 25, and 49 atm), as shown in Fig. 4a. It was observed that as the concentration of draw solute increased, the water flux through the membrane increased, indicating an increase in the driving force for the process. Similarly, an increasing trend was observed for the reverse solute flux. However, 0.5 M NaCl was selected as a draw solution due to high water flux and low-reverse solute flux. Further, it was observed that when GO (0.005 wt.%) was incorporated into the thin-film matrix, the water flux changed from 4.75 to 21.48 LMH at 0.5 M NaCl as the draw solution (Fig. 4b and c). Further, increases in the concentration of GO to 0.01wt.% lead to an average water flux of 26.635 LMH. This increase in water flux for the membrane

Fig. 3 FTIR spectrum and water contact angle of CP, CPT, CPTG, and CPTGC membrane

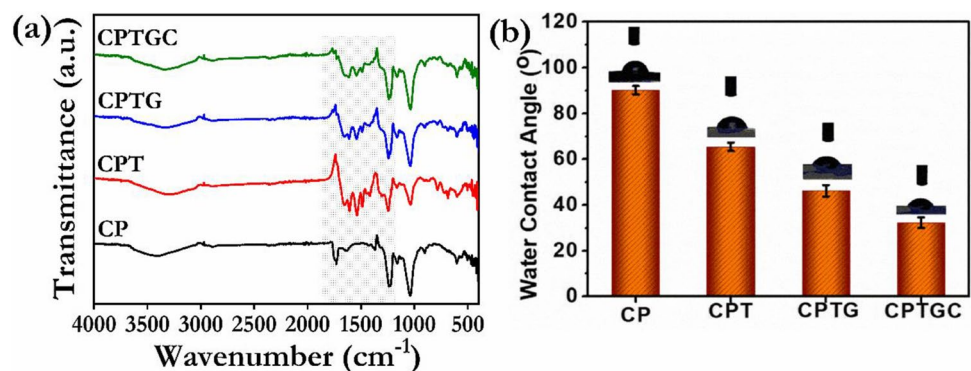
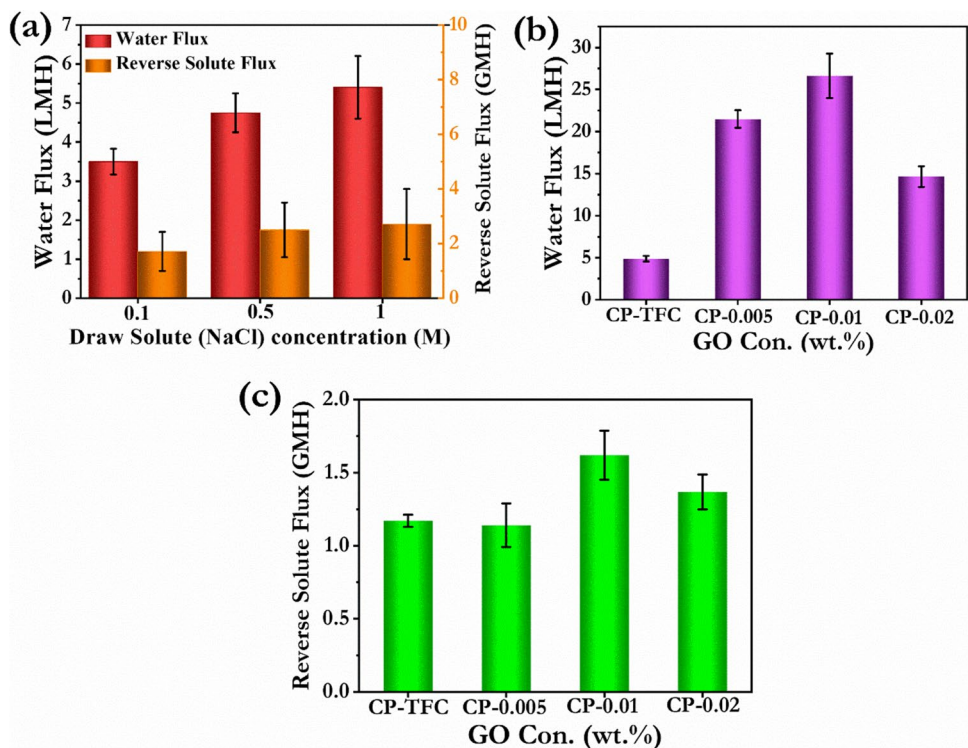


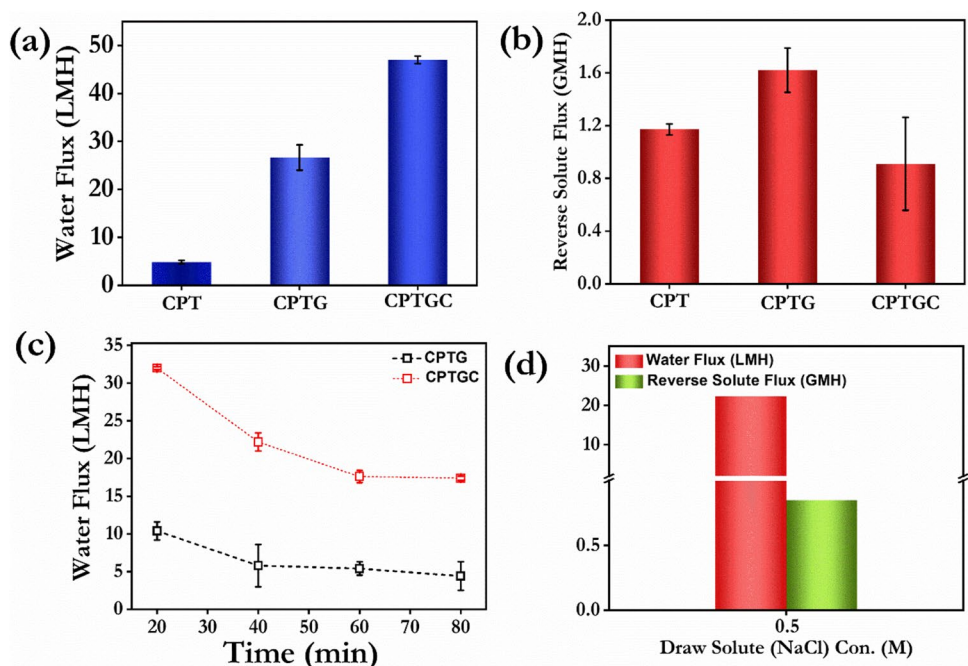
Fig. 4 **a** Water flux and reverse solute flux of CPT membrane at different concentrations of draw solute, **b** water flux, and **c** reverse solute flux of GO incorporated TFC membrane (CPTG)



could be attributed to an increase in the hydrophilicity of the membrane due to the presence of more hydroxyl groups in graphene oxide. After increasing the graphene oxide concentration beyond 0.01 wt.%, a reduction in water flux was observed, which might be because of the fact that a higher concentration of GO could have led to its aggregation in the polyamide layers of the membrane.

The optimized GO (0.01 wt.%)-doped membrane was later assimilated with copper oxide (CuO) on the membrane's same active layers to increase further the hydrophilicity, antifouling, and water flux properties of the membrane. The water flux and reverse solute flux performance comparison of the CP-TFC (CPT), CP-TFC-GO (CPTG), and CP-TFC-GO-CuO (CPTGC) membrane against 0.5 M NaCl as draw

Fig. 5 **a** Water flux and **b** reverse solute flux performance of CPT, CPTG, and CPTGC membrane against 0.5 M NaCl as draw solute, **c** antifouling study for CPTG and CPTGC membranes, and **d** rejection performance for dairy wastewater



solute is shown in Fig. 5a and b. From the figure displayed, it can be concluded that after incorporating both the nanoparticles, the water flux of the membranes increased by a factor of 42. Two batches of fresh laboratory-made dairy wastewater samples were processed by the forward osmosis using a draw solute concentration of 0.5 M NaCl in the AL-FS mode. Firstly, before treating the wastewater, an anti-fouling study was conducted between the only GO-doped and GO-CuO membranes. The better performance membrane could be used for further concentration study. As can be seen from Fig. 5c, the water flux declines rapidly with time for both the membranes, but when the membrane was used again after its washing (conducted inline), it was seen that the GO-CuO-doped membrane was able to recover its flux, then GO-doped membrane. Also, through the literature study, it is found that as the hydrophilicity of the membrane is increased, its capacity to repel the hydrophobic protein increases, thereby increasing the fouling resistance. Therefore, this copper oxide-doped membrane was used for concentrating dairy wastewater (Fig. 5d). The concentration of organic matter in both feed and draw sides were effectively characterized using the TOC (total organic carbon) analyzer. During the FO process conducted for nearly 80 min, the feed concentration increased from ~ 30 to 37 ppm, thus, concentrating the solution up to 23% and a concentration factor of 0.903.

Conclusion

This study investigates the applicability of the novel (CA + PCL) prepared forward osmosis membranes toward concentrating dairy wastewater. After conducting an optimization study for an appropriate blending of two polymers, the membrane was successfully fabricated using phase-inversion methods. Blending PCL into CA significantly improved the mechanical strength of the neat CA membranes. This blended membrane was then effectively modified to prepare a TFC membrane, thereby improving the membrane's hydrophilicity and stability, which resulted in the optimal desired low-reverse solute flux performance of the phase inversion membrane. Further surface modification of this optimized membrane leading to the efficient formation of TFN-integrating graphene oxide and copper oxide with improved hydrophilicity and antifouling properties was used to concentrate the dairy wastewater, positively showing a concentration factor of 0.903.

Acknowledgements The authors would like to thank the Department of Chemical Engineering, National Institute of Technology Calicut (NITC), for the necessary facilities. We would like to thank the Department of Chemistry, NITC for FTIR characterization and CIF-IIT Palakkad for FESEM and WAXD characterization.

Author contribution Akash M. Chandran and Dr. Prasanna Kumar S Mural created the concept and interpreted the data. Ekta Tayal and Akash M. Chandran conducted the literature survey and carried out the experiments. Graphical design and manuscript preparation by Akash M. Chandran.

Funding Authors acknowledge DST-SERB-EEQ/2018/000351 for financial support.

Data availability The information will be provided upon request.

Declarations

Ethics approval Not applicable.

Consent to participate Not applicable

Consent for publication Not applicable.

Competing interests The authors declare no competing interests.

References

- Ayeche R (2012) Treatment by coagulation-flocculation of dairy wastewater with the residual lime of National Algerian Industrial Gases Company (NIGC-Annaba). *Energy Procedia* 18:147–156. <https://doi.org/10.1016/j.egypro.2012.05.026>
- Badawi AK, Zaher K (2021) Hybrid treatment system for real textile wastewater remediation based on coagulation/flocculation, adsorption and filtration processes: performance and economic evaluation. *J Water Process Eng* 40:101963. <https://doi.org/10.1016/j.jwpe.2021.101963>
- Cath TY, Childress AE, Elimelech M (2006) Forward osmosis: principles, applications, and recent developments. *J Membr Sci* 281:70–87. <https://doi.org/10.1016/j.memsci.2006.05.048>
- Chandra R, Castillo-Zacarias C, Delgado P, Parra-Saldívar R (2018) A biorefinery approach for dairy wastewater treatment and product recovery towards establishing a biorefinery complexity index. *J Clean Prod* 183:1184–1196. <https://doi.org/10.1016/j.jclepro.2018.02.124>
- Chandran AM, Varun S, Karumuthil SC et al (2021a) Zinc oxide nanoparticles coated with (3-aminopropyl)triethoxysilane as additives for boosting the dielectric, ferroelectric, and piezoelectric properties of poly(vinylidene fluoride) films for energy harvesting. *ACS Appl Nano Mater* 4:1798–1809. <https://doi.org/10.1021/acsanm.0c03214>
- Chandran AM, Varun S, Mural PKS (2021b) Comparative study on thermal and electrical transport properties of hexagonal boron nitride and reduced graphene oxide/epoxy nanocomposite by transient plane source techniques and impedance spectroscopy. *J Mater Sci Mater Electron* 32:25350–25362. <https://doi.org/10.1007/s10854-021-06994-0>
- Etefagh R, Azhir E, Shahtahmasebi N (2013) Synthesis of CuO nanoparticles and fabrication of nanostructural layer biosensors for detecting *Aspergillus niger* fungi. *Sci Iran* 20:1055–1058. <https://doi.org/10.1016/j.scient.2013.05.015>
- He N, Li L, Chen J et al (2021) Extraordinary superhydrophobic polycaprolactone-based composite membrane with an alternated micro-nano hierarchical structure as an eco-friendly oil/water separator. *ACS Appl Mater Interfaces* 13:24117–24129. <https://doi.org/10.1021/acsami.1c03019>

- Joshi MK, Tiwari AP, Pant HR et al (2015) In situ generation of cellulose nanocrystals in polycaprolactone nanofibers: effects on crystallinity, mechanical strength, biocompatibility, and biomimetic mineralization. *ACS Appl Mater Interfaces* 7:19672–19683. <https://doi.org/10.1021/acsami.5b04682>
- Khoshnevisan K, Maleki H, Samadian H et al (2019) Antibacterial and antioxidant assessment of cellulose acetate/polycaprolactone nanofibrous mats impregnated with propolis. *Int J Biol Macromol* 140:1260–1268. <https://doi.org/10.1016/j.ijbiomac.2019.08.207>
- Liu C, Li X, Liu T et al (2016) Microporous CA/PVDF membranes based on electrospun nanofibers with controlled crosslinking induced by solvent vapor. *J Membr Sci* 512:1–12. <https://doi.org/10.1016/j.memsci.2016.03.062>
- Loeb S, Sourirajan S (1963) Sea water demineralization by means of an osmotic membrane. In: *Saline Water Conversion—II*. American Chemical Society, pp 117–132. <https://doi.org/10.1021/ba-1963-0038.ch009>
- Maior A, Gammino M, Gulino EF et al (2020) Rapid one-step fabrication of graphene oxide-decorated polycaprolactone three-dimensional templates for water treatment. *ACS Appl Polym Mater* 2:4993–5005. <https://doi.org/10.1021/acsapm.0c00852>
- Mural PKS, Sharma M, Shukla A et al (2015) Porous membranes designed from bi-phasic polymeric blends containing silver decorated reduced graphene oxide synthesized via a facile one-pot approach. *RSC Adv* 5:32441–32451. <https://doi.org/10.1039/C5RA01656H>
- Obaid M, Ghouri ZK, Fadali OA et al (2016) Amorphous SiO₂ NP-incorporated poly(vinylidene fluoride) electrospun nanofiber membrane for high flux forward osmosis desalination. *ACS Appl Mater Interfaces* 8:4561–4574. <https://doi.org/10.1021/acsami.5b09945>
- Palacios Hinestroza H, Urena-Saborio H, Zurita F et al (2020) Nanocellulose and polycaprolactone nanospun composite membranes and their potential for the removal of pollutants from water. *Molecules* 25:683. <https://doi.org/10.3390/molecules25030683>
- Park HM, Jee KY, Lee YT (2017) Preparation and characterization of a thin-film composite reverse osmosis membrane using a polysulfone membrane including metal-organic frameworks. *J Membr Sci* 541:510–518. <https://doi.org/10.1016/j.memsci.2017.07.034>
- Pramanik BK, Hai FI, Roddick FA (2019) Ultraviolet/persulfate pretreatment for organic fouling mitigation of forward osmosis membrane: possible application in nutrient mining from dairy wastewater. *Sep Purif Technol* 217:215–220. <https://doi.org/10.1016/j.seppur.2019.02.016>
- Riaz T, Ahmad A, Saleemi S et al (2016) Synthesis and characterization of polyurethane-cellulose acetate blend membrane for chromium (VI) removal. *Carbohydr Polym* 153:582–591. <https://doi.org/10.1016/j.carbpol.2016.08.011>
- Rouhani ST, Fashandi H (2018) Breathable dual-layer textile composed of cellulose dense membrane and plasma-treated fabric with enhanced comfort. *Cellulose* 25:5427–5442. <https://doi.org/10.1007/s10570-018-1950-9>
- Slavov AK (2017) General characteristics and treatment possibilities of dairy wastewater – a review. *Food Technol Biotechnol* 55:14–28. <https://doi.org/10.17113/ftb.55.01.17.4520>
- Sun Y, Wang Q, Zhang S et al (2018) Synthesis of aromatic-doped polycaprolactone with tunable degradation behavior. *Polym Chem* 9:3931–3943. <https://doi.org/10.1039/C8PY00374B>
- Tufa RA, Di Profio G, Fontananova E, et al (2019) Chapter 15 - Forward osmosis, reverse electrodialysis and membrane distillation: new integration options in pretreatment and post-treatment membrane desalination process. In: Basile A, Curcio E, Inamuddin (eds) *Current trends and future developments on (Bio-) Membranes*. Elsevier, pp 365–385
- Xue W, Tobino T, Nakajima F, Yamamoto K (2015) Seawater-driven forward osmosis for enriching nitrogen and phosphorous in treated municipal wastewater: effect of membrane properties and feed solution chemistry. *Water Res* 69:120–130. <https://doi.org/10.1016/j.watres.2014.11.007>
- Zhang S, Wang KY, Chung T-S et al (2010) Well-constructed cellulose acetate membranes for forward osmosis: minimized internal concentration polarization with an ultra-thin selective layer. *J Membr Sci* 360:522–535. <https://doi.org/10.1016/j.memsci.2010.05.056>
- Zhang X, Zhao J, Ma L et al (2019) Biomimetic preparation of a polycaprolactone membrane with a hierarchical structure as a highly efficient oil–water separator. *J Mater Chem A* 7:24532–24542. <https://doi.org/10.1039/C9TA08660A>

Publisher's note Springer Nature remains neutral with regard to jurisdictional claims in published maps and institutional affiliations.